

1 Research paper

2 **Temperature and Solvent Facilitated Extrusion (TASFEX) Based**  
3 **3D Printing for Pharmaceuticals**

4

5

6

7

8

9

10

11

12 Filipa Dores<sup>1</sup>, Magda Kuźmińska<sup>1,2</sup>, Cindy Soares<sup>1</sup>, Leroy Shiverington<sup>1</sup>, Rober Habashy<sup>1</sup>,  
13 Matthew Peak<sup>3</sup>, Abdullah Isreb<sup>1</sup>, Mohamed A Alhnan<sup>4\*</sup>

14

15

16

17

18

19 <sup>1</sup>*School of Pharmacy and Biomedical Sciences, University of Central Lancashire, Preston, Lancashire, UK*

20 <sup>2</sup>*Faculty of Pharmacy with the Laboratory Medicine Division, Medical University of Warsaw, Warsaw, Poland.*

21 <sup>3</sup>*Paediatric Medicines Research Unit, Alder Hey Children's NHS Foundation Trust, Liverpool, UK*

22 <sup>4</sup>*Institute of Pharmaceutical Sciences, King's College London, London, UK.*

23

24 **ABSTRACT**

25 On demand manufacturing of patient-specific oral doses provides significant advantages to patients and  
26 healthcare staff. Several 3D printing (3DP) technologies have been proposed as a potential digital  
27 alternative to conventional manufacturing of oral tablets. For additive manufacturing approach to be  
28 successful for on-demand preparation, a facile process with minimal preparation steps and training  
29 requirements is needed. A novel hybrid approach to the 3D printing process is demonstrated here based  
30 on combined solvent and heating elements/factors/aspects to facilitate extrusion. The system employed  
31 a moderate elevated temperature range of (65-100 °C), a brief drying period, and a simple set-up. In this  
32 approach, a compact powder cylinder is used as a pharmaceutical ink to be extruded in a temperature-  
33 controlled metal syringe. The process proved compatible with hygroscopic polymers [Poly(vinyl  
34 alcohol (PVA) and poly(vinyl pyridine) (PVP)] and a number of pharmaceutical fillers (lactose,  
35 sorbitol and mannitol). The fabricated tablets demonstrated compendial acceptable weight and content  
36 uniformity as well as mechanical resistance. In vitro drug release of theophylline from 3D printed tablets  
37 was dependant on the nature of the polymer and its molecular weight. This reported approach offers  
38 significant advantages compared to other 3DP technologies: simplification of pre-product, the use of a  
39 moderate temperature range, a minimal drying period, and avoiding the use of mechanically  
40 complicated direct extruder machinery. In the future, we envisage the use of this low-cost and facile  
41 approach to fabricate small batches of bespoke tablets.

42

43

44 *Keywords:* Direct Ink writing, personalized, patient-specific, small batch, early phase clinical trials

## 45        **1. Introduction**

46        The demand for personalised therapies has been increasing over the last decade due to the most recent  
47        advances in pharmacogenomics and stratified medicine. This has allowed complex diseases and their  
48        biological mechanisms to be better understood and to develop more effective strategies to predict and  
49        prevent illnesses, as well as to treat them [1-3]. Such developments in personalised therapies induced  
50        the interest in developing digital solutions for small batch production of patient-specific dosage forms  
51        [4, 5].

52        The past few years have witnessed a growing interest in 3D printing (3DP) as an on-demand  
53        manufacturing tool for small batch manufacturing, age-specific products in paediatrics [6, 7] and  
54        meeting the needs of polypharmacy [8-10]. With several 3DP technologies available, fused deposition  
55        modelling (FDM) 3DP has been proposed as a low-cost solution for the fabrication of patient specific  
56        dosage forms [11-16]. The FDM technology offers significant potential advantages including process  
57        simplicity, the lack of drying or finishing steps and potential of mass production of low-cost  
58        pharmaceutical printers and ink cartridges. However, FDM 3DP has to overcome some significant  
59        technical challenges to wider uptake and adoption as it exposes the starting pharmaceutical material to  
60        two sequential-thermal processes (when hot melt extrusion-based filaments are used as a feed) [5, 17],  
61        engineering and optimizing the ‘feedability’ of the filament [18-20], as well as minimising the risk of  
62        mechanical and physical modification of the filament during storage prior to on-demand 3DP. Such  
63        challenges might hinder or slow down the advances of this important technology in the pharmaceutical  
64        market. Several modifications to FDM 3DP have been applied to reduce the thermal stress of the  
65        printing process. For instance, Okwuosa et al. [21] pioneered the use of poly(vinyl alcohol) (PVA) to  
66        reduce the printing temperature to as low as 110 °C. Other adaptations have further reduced the printing  
67        temperature by employing polymers with low glass transition temperature (90 °C) [22], by the  
68        replacement of filaments with softer extruded polymer strands as low as 54 °C [23, 24], or by using  
69        water in filament preparation step as a temporary plasticiser [9].

70        Extrusion-based 3DP has been proposed as an alternative method of manufacture of tablets. While the  
71        former obviates the need of engineering and stabilising filaments, it faces a major challenge of extruding  
72        a material into solidifying structures in acceptable time. The extrusion of semi-solids (drug suspension)  
73        at room temperature can be employed using a printer often used in tissue engineering [10, 25-27]. The  
74        process involves the use of powder slurry in a significant amount of water [25, 27, 28] or ethanol [29].  
75        By using thermally heated piston-operated syringe (<70 °C), extrusion-based 3D printing was also  
76        employed to produce solid self-micro-emulsifying drug delivery systems [30] and chewable jelly-like  
77        tablets [31]. Alternatively, extrusion can be carried out at high temperature with built-in screw extruder  
78        [32]. However, this promising technology must overcome several barriers such balancing efficient  
79        extrusion process with the use of typically heavy machinery (hot extruder motor assembly) that are

80 often needed to provide sufficient torque for extrusion as well as providing easy solution for batch-to-  
81 batch cleaning of complex-shaped screws in the extruder assembly.

82 In this paper, we present the use of a novel alternative approach of temperature and solvent facilitated  
83 extrusion-based 3D printing as a facile manufacturing process suitable for extemporaneous preparations  
84 near to the patient. This hybrid approach of combining solvent and elevated temperature for fabrication  
85 of oral tablets uses an extrusion-based system that is delivered by simple metal syringe. We envisage  
86 the use of a compressed powder cylinder as a pharmaceutical ink.

## 87 **2. Materials and methods**

### 88 *2.1 Materials*

89 Theophylline was purchased from Acros Organics (UK). Three grades of Poly(vinyl alcohol) were used:  
90 PVA 20-30K and PVA 83K were supplied from Fisher scientific UK, and PVP Parateck® MXP [MXP,  
91 k75] was donated by Merck (Darmstadt, Germany). Polyvinylpyrrolidone (PVP, Plasdone™ K-29/32)  
92 was donated by Ashland (UK). Sodium stearyl fumarate (PRUV) was donated by JRS (Germany) and  
93 sorbitol was purchased from Merck (Parateck SI, Germany). D-mannitol, lactose and HPLC gradient  
94 grade acetonitrile were obtained from Fisher Scientific Ltd (Loughborough, UK).

### 95 *2.2 Preparation for the feed*

96 The model drug (theophylline) and polymer (PVA 20-30K, Parateck [MXP, k75], PVA 83K, PVP) in  
97 addition to other additives were accurately weighed and thoroughly mixed via shear mixing using Krups  
98 F20342 grinder (Germany). The breakdown of each blend compositions is detailed in Table 1. Initially,  
99 sorbitol was selected as a primary plasticiser as established plasticising capacity for PVA matrixes [33,  
100 34] and structure enhancer. Lactose and D-mannitol were added for common use as highly soluble  
101 structure enhancers [35, 36]. Preliminary screening work indicated that material flow from the syringe  
102 could be significantly enhanced by the addition of sodium stearyl fumarate at 5% as a lubricant. Further  
103 increase in of sodium stearyl fumarate led to incomplete 3D printing due to poor adhesion of the tablet  
104 to the printing plate or weak fusion of the printed layers. To approximately 10 g of each blend, an  
105 additional 2 g of deionised water was added to each formulation and mixed for an additional 30 seconds.  
106 Each blend was compressed using a 12 mm diameter metal syringe (Hyrel 3D, Atlanta, USA) to form  
107 10 cm height cylinder. The compressed cylinder (based on 12 g of polymer blend + water) were stored  
108 in plastic polybag and used as feed for the 3D printing process (Section 2.3).

109 In order to assess the impact of the filler nature, sorbitol was replaced with an equivalent amount of D-  
110 mannitol or lactose. To assess the impact of different plasticiser concentrations of sorbitol: 15%, 20%  
111 and 25% (w/v) were assessed. Table 1 provides a summary of all formulations prepared using TASFEX  
112 technology.

### 113 2.3 Tablet design and TASFEX 3D printing

114 The tablets were designed in a cylindrical shape using Autodesk® 3ds Max Design 2019 (Autodesk,  
115 Inc., USA). The designs were then imported to the Slic3r (version 1.3) software in stereolithographic  
116 (STL) format and converted to gcode files using the settings specified as: layer thickness 0.3 mm, first  
117 layer thickness 0.5 mm, speed perimeters 50%, infill speed 7 mm/sec, travel speed 15 mm/sec, first  
118 layer build speed 7 mm/sec, and nozzle diameter 1.19 mm.

119 A Hyrel System 30M (Hyrel 3D, Atlanta, USA) equipped with a VOL-25 (Volcano) modular head and  
120 a 16-gauge stainless steel tip was used to fabricate the tablets. The default glass plate was replaced with  
121 an acrylic sheet for better adhesion to the building plate. The settings inserted in the Repetrel software  
122 (version 3.0) for the printer head were: nozzle diameter: 1.194, thickness of layer z: 0.3 mm, motor  
123 pulses rate: 2.3 pulses/nL, infill percentage: 100% and a material flow multiplier: 1.2. Following the  
124 printing process the tablets were dried for 2 hours at 50 °C using Binder Drying chamber 9010 (Binder  
125 GmbH, Germany). Prior to printing, the compressed cylinder was placed in the heated syringe and  
126 heated at processing temperature for 30 min.

### 127 2.4 Thermal analysis

128 Samples of the raw materials, dry physical mixture and 3D printed tablets were analysed by differential  
129 scanning calorimetry (DSC) and thermogravimetric analysis (TGA). DSC Q2000 (TA Instruments,  
130 Elstree, UK) was used to assess the thermal behaviour of the samples: approximately 5 mg samples  
131 were scanned from 0 to 300°C using at a heating rate of 10°C/min and a nitrogen purge of 50 mL/min  
132 using standard aluminium pans and lids. TGA Q500 (TA Instruments, Elstree, Hertfordshire, UK) was  
133 used to analyse approximately 10 mg of each material filled in platinum pans. Samples were heated at  
134 a rate of 10°C/min from 25°C to 500°C with a nitrogen purge of 40:60 ml/min for sample: furnace  
135 respectively. TA Universal analysis software (v 4.5A, TA Instruments, Elstree, UK) was used to analyse  
136 data for both DSC and TGA.

### 137 2.5 X-Ray Diffractometry (XRD)

138 A powder X-ray diffractometer, D2 Phaser with Lynxeye (Bruker, Germany) was used to assess the  
139 physical form of the model drug and fillers within the 3D printed tablets. Samples were scanned from  
140  $2\theta = 5^\circ$  to  $50^\circ$  using  $0.01^\circ$  step width and a 1.25 s time count. The divergence slit was 1 mm and  
141 the scatter slit 0.6 mm. The wavelength of the X-ray was 0.154 nm using Cu source and a voltage of  
142 30 kV. Filament emission was 10 mA using a scan type coupled with a theta/theta scintillation counter  
143 over 60 min.

### 144 2.6 Water contents

145 The water content was determined using Karl Fischer method (KF) using Metrohm 870 KF Titrino plus  
146 (Metrohm UK Ltd., Runcorn, UK). Each ingredient and dried 3D printed tablets has been measured  
147 sample (500 mg) accurately weight using Mettler Toledo analytical balance (Mettler, Germany). The  
148 water content was calculated via Titrino plus software (Metrohm UK Ltd., Runcorn, UK) or end-point  
149 was utilized for % water content calculation.

150

### 151 *2.7 Dimensions and mechanical properties of the 3D printed tablet*

152 To assess the mechanical resistance of 3D printed tablets, the 3D printed tablets were assessed  
153 using Agilent 200 Tablet Hardness Tester (Agilent Technologies). Measurements of resistance  
154 to crushing of the tablet were carried out in triplicates for each selected formulation. The  
155 friability of 3D printed tablets (n=10) were accurately weighed, placed in the apparatus drum  
156 of Agilent Dual-drum Friability Tester 250 (Agilent Technologies) and rotated 100 times. The  
157 dimensions of 3D tablet dimensions were assessed using eSYNdic Digital Vernier digital  
158 calliper (eSYNdic, China). A randomly selected 10 3D printed tablets from each selected  
159 formulation were and weighed. The average mass, standard deviation and percentage deviation  
160 from average mass were determined for each batch.

### 161 *2.8 Analysis of drug contents using HPLC*

162 Theophylline content of the tablets was assessed using an Agilent 1260 series UV-HPLC  
163 (Agilent Technologies, Germany) with XTerra RP 18 column (150 × 4.6 mm, 5 µm particle  
164 size) (Waters, Ireland) as previously reported [21]. The mobile phase (86:7:7 volume ratio of  
165 10 mM ammonium acetate buffer: methanol: acetonitrile) was applied at flow rate of 1 mL/min  
166 at temperature 40°C. Samples were injected (5 µL) and the run time of 7 min and analysis was  
167 carried out at a wavelength of 272 nm.

### 168 *2.9 Scanning Electron Microscopy (SEM)*

169 The morphology and cross-section of the tablets were assessed using a JCM-6000 plus  
170 NeoScope™ microscope (Jeol, Tokyo, Japan) at 10 kV. All samples were gold coated using a  
171 JFC-1200 Fine Coater (Jeol, Tokyo, Japan). The images were collected using Image J software  
172 (v 1.2.0., Tokyo, Japan).

### 173 *2.10 In vitro disintegration and dissolution*

174 *In vitro* disintegration and drug release studies. Tablet disintegration was carried out using an  
175 Erweka ZT220 disintegration testing apparatus (Erweka GmbH, Heusenstamm, Germany).

176 Three tablets were randomly selected, weighed and each placed in a basket rack assembly of  
177 six cylinders and weights were added on the top of the tablets. The basket rack assembly was  
178 then immersed into a beaker containing 0.1M hydrochloric acid at 37 °C. The exact time for all  
179 tablets to fully leave the mesh was visually noted.

180 *In vitro* drug release testing. The impact of the tablet's design on the release pattern of the 3D  
181 printed tablets was assessed using a USP II dissolution test paddle apparatus (Erweka GmbH,  
182 Germany). The dissolution study was conducted in 900 mL of 0.1 M hydrochloric acid (pH  
183 1.2) at  $37 \pm 0.5$  °C and with paddle speed of 50 rpm. The amount of released theophylline was  
184 determined at 5 min intervals by UV/VIS spectrophotometer (PG Instruments Limited, UK) at  
185 a wavelength of 272 nm and a path length of 1 mm. Data were analysed using IDISis software  
186 version 2012 (Automated Lab, Berkshire, UK).

### 187 **3. Results and Discussion**

188 The manufacturing equipment required for TASFEX is illustrated in **Fig. 1**. Here, a  
189 cylinder of compressed pharmaceutical ink is loaded into a metal syringe and water is added.  
190 The material is pressurised under a moderately elevated temperature (50-100°C) using the  
191 support of a piston stepper motor with a built-in gear to increase the load-to-motor inertia ratio  
192 and to reduce motor oscillation. In this arrangement, the starting material can be loaded as a  
193 compressed powder in a form of cylinder (12mm diameter x 60 mm height) to produce a set  
194 number of tablets. The simplicity of this set-up and the lack of screw parts of complicated  
195 design that necessitate special cleaning protocols make it particularly suitable for dispensing  
196 bespoke doses in a hospital setting. In the future, it is possible to employ low-cost thermally  
197 conductive disposable syringes to eliminate the risk of cross-contamination for production of  
198 multiple batches.

199 Initially, tablet extrusion was carried out without the inclusion of water. However, no  
200 material flow was possible at the process temperature of 90°C. Preliminary investigations  
201 indicated that a significant increase of the plasticiser (sorbitol) ratio allow significant material  
202 flow. However, this approach led to the formation of a highly flexible matrix that was not  
203 suitable for oral tablet structure (data not shown). Here, we adapted the solution of adding water  
204 as a temporary plasticiser as previously reported [9]. In this approach, water was added to the  
205 final powder blends to facilitate the printing of these tablets. **Table 1** shows the content of  
206 different formulations which were prepared using the novel TASFEX system. The inclusion of  
207 water allowed a sufficient material flow from the temperature-controlled metal syringe and

208 enabled 3D printing at relatively low temperature (65-100°C). The concentration of plasticiser  
209 (sorbitol) was varied in the presence of a fixed amount of water and the fabrication process was  
210 successful in a sorbitol concentration range of 15-25% w/v. A filler ratio of 20% was chosen,  
211 as it yielded the most visually desirable structure of a smooth surface and a consistent filling.  
212 In order to assess the suitability of the process to different fillers, two additional sugars (lactose  
213 and D-mannitol) were incorporated in the formulation which yielded well-structured tablets  
214 demonstrating the versatility of the process (**Figs. 2 a1-d1**).

215 SEM images indicated the formation of relatively smooth upper surface of tablets (**Figs.**  
216 **2 a2-d2**). Each layer was composed of 300µm layers (**Figs. 2 a3-d3**). Interestingly, the SEM  
217 images of the cross-sections of the tablet indicated that PVA-based tablet made with lactose  
218 and D-mannitol showed individual layers, tablets that are based on PVA-sorbitol and PVP-  
219 lactose demonstrated a more cohesive structure with seamless lines between the deposited  
220 layers (**Figs. 2 a4-d4**).

221 The TGA thermograph showed that all molecules were stable at the processing  
222 temperature ( $\leq 100$  °C) (**Fig. 3**). In all these examples, the 3D printed tablets appeared to lose  
223 approximately <3% of their total mass due to moisture evaporation. The magnitude of this loss  
224 is significantly lower in the powder blend (physical mixture) in comparison to the 3D printed  
225 tablets, indicating that these tablets retained some level of water. To assess the impact of drying  
226 process, Karl Fisher analysis was used to assess the percentage of moisture content in the dried  
227 3D printed tablets **Table S1 (Supplementary data)**. The analysis indicated that drying process  
228 yielded 3D printed tablet (F2) of minimal water contents (<0.5%). While this approach offers  
229 advantages over using highly diluted drug and additive slurry [25, 27, 28] and producing  
230 relatively solid structure before any additional drying process, the elevated processing  
231 temperature might be less suitable for thermally labile drug.

232 DSC thermographs indicated that onset of melting points of sorbitol, lactose and  
233 mannitol of 91, 140 and 164 °C respectively [37]. The physical blend indicated the presence of  
234 these peaks in their corresponding thermographs. When the 3D printed tablets were tested,  
235 minor or no endothermic peak were seen in sorbitol tablets (n=3) (**Fig. 4a**), whilst the  
236 endothermic melting peaks were clearer in both D-mannitol and lactose thermographs (**Figs. 4b,**  
237 **4c**). The role of sorbitol as a plasticiser has been described before in PVA matrix [38]. The  
238 significant ability of this sugar to plasticise PVA matrix was directly related to its ability to  
239 form hydrogen bonds with -hydroxyl groups of PVA structure as well as water molecules,



240 hence enhancing the polymer ability to retain water [39]. These findings suggest that lactose  
241 and mannitol might be less miscible within the PVA matrix and therefore a significant portion  
242 of the sugar were in the crystalline form within the 3D printed structure.

243 XRD intensity patterns indicated that sorbitol (as received) has distinctive intensity  
244 peaks of  $2\theta = 12.12^\circ$  and  $19.1^\circ$  (**Fig. 5a**). While these peaks appeared in the physical  
245 mixture, they were absent in the XRD patterns of the 3D printed tablets, and hence confirmed  
246 that sorbitol was mainly in the amorphous form within the 3D printed tablet matrix. However,  
247 in the case of lactose ( $2\theta = 16.4^\circ$ ) and D-mannitol ( $2\theta = 16.9, 35.9$  and  $44.13^\circ$ )  
248 suggesting that both fillers were in crystalline form (**Figs. 5 b and c**). This could be the result  
249 of applying processing temperatures (90-100 °C) that reached the melting point of sorbitol (91  
250 °C), but below the melting point of lactose and D-mannitol (140 and 164 °C). The presence of  
251 both lactose and D-mannitol in crystalline form might have favoured the formation of tablets  
252 of improved physical structure. XRD patterns also indicated that theophylline was in crystalline  
253 form with the presence of peaks  $2\theta = 6.8$  and  $12.3^\circ$  (**Figs. 5 a, b and c**).

254 The extrudability of the polymeric matrix can be linked to its rheological behaviour.  
255 The complex viscosity of the material were observed to drop down when polymer was blended  
256 with other non-melting additives [40, 41]. It was noticed that the glass transition temperature  
257 ( $T_g$ ) dropped with the decrease in the complex viscosity of the mixture [41]. In another  
258 example, the addition of sugar (lactose, mannitol, or sorbitol) to polyethylene glycol matrix  
259 was noticed to help in controlling the complex viscosity [42] by maintaining a shear-thinning  
260 behaviour, which is required for extrudability followed by solidification at room temperature.

261 In order to demonstrate the versatility of the presented method to accommodate  
262 different polymer species, pyrrolidine derivative (PVP) was also tested as a polymer species  
263 and yielded a tablet (**Fig. 2f**). Physical analysis indicated that lactose was in the crystalline  
264 form (endotherm of melting peak onset at 140 °C and an intensity peak XRD patterns ( $2\theta = 16.4^\circ$ )  
265 (**Fig. 6**). However, when less hydrophilic polymers (e.g. Eudragit E, Eudragit L,  
266 Eudragit EPO or HPC SL) were applied in the same formulation, the solvent (water) separated  
267 from the powder bulk (Eudragit E and HPC SL) or the extruded filaments from hot nozzle  
268 failed to fuse together following application from the nozzle to yield a cohort 3D structure.  
269 This demonstrates that the reported TASFEX approach is more suitable for polymer systems  
270 with functional groups of hydrophilic properties which are able to retain water within the  
271 polymeric matrix and facilitates multilayer adhesion upon hydration.

272 Four selected formulations were selected for further tablet characterization as detailed  
273 in **Table 2**. The pharmacopeial tests indicated a generally long disintegration time for 3D  
274 printed tablet structures. This is in agreement with recent reports in which polymer-rich 3D  
275 printed structures showed slow *in vitro* dissolution profiles despite the use of fast-dissolving  
276 polymers that are typically used for immediate release preparations [32, 43]. This in contrast  
277 to immediate release and fast disintegrating tablets are often composed with large portion of  
278 disintegrating fillers. The disintegration time was reported to be much shorter for the D-  
279 mannitol based tablet (**Table 2**) compared to other fillers. Such disintegrants effect of D-  
280 mannitol has been previously reported [44, 45].

281 Despite the relatively large nozzle size used for the extrusion of polymeric structure  
282 (1.2 mm), the majority of fabricated tablets illustrated highly reproducible dimensions and  
283 weight (**Table 2**). The tablets also demonstrated pharmaceutically acceptable mechanical  
284 properties of friability (<1%). The *in vitro* dissolution of the fabricated tablets is shown in **Fig.**  
285 **7**. Modifying the percentage of sorbitol in the PVA matrix appeared to have a limited impact  
286 of the rate of theophylline release (**Fig. 7a**). The nature of dissolution seems also to be  
287 independent of the nature of the plasticiser sugar (**Fig. 7b**). This indicates that the theophylline  
288 release was mainly dominated by the erosion of PVA. As the dissolution medium penetrate  
289 through PVA matrix, drug release will take place through the erosion of the hydrate matrix and  
290 diffusion through the polymeric chain networks [46]. When other PVA grades with higher and  
291 lower molecular weight were incorporated in the tablets, drug release was dependent on the  
292 molecular weight of the PVA grade (**Fig. 7c**). This observation can be attributed to the  
293 reduction of water diffusion co-efficient with increased molecular weight of PVA [47]. On the  
294 other hand, the use of PVP as a base for 3D printed tablets resulted in theophylline release of  
295 >85% at 45 min in the gastric medium (**Fig. 7d**) and was compatible with the BP pharmacopeia  
296 for immediate release theophylline tablets. The fast dissolution rate from PVP matrix could be  
297 attributed to its solubility enhancing properties [48, 49]. Drug release from 3D printed tablets  
298 seemed to mimic that from tablets produced via FDM 3D printing [21, 24, 50]. Upon  
299 introduction to aqueous media, the polymer-rich structure of these tablets resulted in formation  
300 of gel-like layer [51]. Further acceleration to drug release could be achieved through design  
301 approach [43].

302 Despite the significant advances of the reported approach, it is confined to small batch  
303 manufacturing and is less suitable for large scale or continuous manufacturing. Although  
304 drying time is relatively brief, the combination of heat and water might accelerate drug

305 degradation particularly if hydrolysis-labile molecule is incorporated. The omittance of the  
306 drying process could be achieved by avoiding the use of solvent, however, this will involve use  
307 of high processing temperature or materials of low melting points. This highlights the  
308 importance of carefully selecting the 3D printing manufacturing approach to suit a particular  
309 active molecule and batch size.

#### 310 **4. Conclusion**

311 We have reported a novel hybrid approach of combined temperature and solvent (water) to  
312 facilitate the additive manufacturing of immediate release tablets using simple extrusion. The  
313 proposed process was compatible with pharmaceutical grade hygroscopic polymers (PVA and  
314 PVP). We demonstrated that the starting material was compatible with a number of fillers  
315 (lactose, sorbitol and D-mannitol). The produced tablets demonstrated pharmacopeial  
316 acceptable weight and content uniformity and proved mechanically resistant. This reported  
317 hybrid approach offers significant advantages compared to other 3DP technologies: i)  
318 replacing difficult-to-engineer FDM -compatible filament with a simpler powder or compact  
319 cylinder, ii) the use of a moderate temperature range (65-100 °C), iii) a brief drying period, and  
320 iv) avoiding the use of mechanically complicated and hard-to-clean direct extruder machinery.  
321 These novel features can provide hospital and compounding units with a simple, low-cost  
322 approach to dispense small batch of patient-customised tablets. However, for continuous  
323 manufacturing, removal of drying step, and hydrolysis labile drugs, other manufacturing  
324 approach could be considered.

325

326

327 **List of Figures:**

328

329 **Fig. 1.** Equipment for TASFEX 3D printing. (a) The printer is equipped with a metal syringe surrounded  
330 by temperature-controlled heating jacket. The syringe is fitted with a luer-lock stainless steel needle,  
331 (b) The pharmaceutical ink (compressed powder) is added. The ink is then extruded by a piston pushed  
332 by computer-controlled stepper motor equipped with gear to produce (c) 3D printed tablet.

333 **Fig. 2** Photographs of 3D printed tablets based on (a1) PVA and sorbitol, (b1) PVA and lactose and  
334 (c1) PVA and D-mannitol and (d1) PVP and lactose. SEM images of (a2, b2, c2 and d2) top view, (a3,  
335 b3, c3 and d3) side view, and (a4, b4, c4 and d4) cross sections of these tablets.

336 **Fig. 3** TGA thermal degradation profiles of raw theophylline, PVA, Sodium stearyl fumarate (PRUV),  
337 filler [ (a) sorbitol, (b) lactose and (c) D-mannitol], pharmaceutical ink (prior to addition of water) and  
338 3D printed tablets.

339 **Fig. 4** DSC thermograph of raw theophylline, PVA, Sodium stearyl fumarate (PRUV), filler [(a)  
340 sorbitol, (b) lactose and (c) D-mannitol], pharmaceutical ink (prior to addition of water) and 3D printed  
341 tablets.

342 **Fig. 5** XRD patterns of raw theophylline, PVA, Sodium stearyl fumarate (PRUV), filler [ (a) sorbitol,  
343 (b) lactose and (c) D-mannitol, pharmaceutical ink (prior to addition of water) and 3D printed tablets.

344 **Fig. 6** 3D Printed tablet based on poly(vinylpyridine) (PVP) (A) TGA thermal degradation profiles, (B)  
345 DSC thermograph profiles, (C) XRD patterns of raw theophylline, PVP, Sodium stearyl fumarate  
346 (PRUV), lactose, pharmaceutical ink (prior to addition of water) and 3D printed tablets.

347 **Fig. 7** Impact of (a) sorbitol percentage, (b) nature of filler (sorbitol, lactose and D-mannitol), and (c)  
348 molecular weight of PVA on the *in vitro* dissolution of theophylline from 3D printed tablets, (d) *in vitro*  
349 dissolution of theophylline from 3D printed PVP based tablets ( $n=3, \pm SD$ ).

350 **List of tables**

351 **Table 1** Composition of materials used in TASFEX, extrusion and plate temperatures

352 **Table 2** Diameter, height, weight uniformity, friability, hardness, disintegration and drug content.

353 **Supplementary Data**

354 **Table S1** Water content of ingredients, physical mixture, freshly prepared and dried 3D printed tablet  
355 based on sorbitol and PVA

356 **References**

- 357 [1] W. Burke, H. Burton, A.E. Hall, M. Karmali, M.J. Khoury, B. Knoppers, E.M. Meslin, F. Stanley, C.F.  
358 Wright, R.L. Zimmern, G. Ickworth, Extending the reach of public health genomics: what should be  
359 the agenda for public health in an era of genome-based and "personalized" medicine?, *Genet Med*,  
360 12 (2010) 785-791.
- 361 [2] A. Alyass, M. Turcotte, D. Meyre, From big data analysis to personalized medicine for all:  
362 challenges and opportunities, *BMC Med Genomics*, 8 (2015) 33.
- 363 [3] J. Savard, Personalised medicine: a critique on the future of health care, *J Bioeth Inq*, 10 (2013)  
364 197-203.
- 365 [4] M.A. Alhnan, T.C. Okwuosa, M. Sadia, K.W. Wan, W. Ahmed, B. Arafat, Emergence of 3D Printed  
366 Dosage Forms: Opportunities and Challenges, *Pharm Res*, 33 (2016) 1817-1832.
- 367 [5] A. Awad, S.J. Trenfield, S. Gaisford, A.W. Basit, 3D printed medicines: A new branch of digital  
368 healthcare, *Int J Pharm*, 548 (2018) 586-596.
- 369 [6] H. Oblom, E. Sjöholm, M. Rautamo, N. Sandler, Towards Printed Pediatric Medicines in Hospital  
370 Pharmacies: Comparison of 2D and 3D-Printed Orodispersible Warfarin Films with Conventional Oral  
371 Powders in Unit Dose Sachets, *Pharmaceutics*, 11 (2019).
- 372 [7] N. Scoutaris, S.A. Ross, D. Douroumis, 3D Printed "Starmix" Drug Loaded Dosage Forms for  
373 Paediatric Applications, *Pharm Res*, 35 (2018) 34.
- 374 [8] P. Robles-Martinez, X. Xu, S.J. Trenfield, A. Awad, A. Goyanes, R. Telford, A.W. Basit, S. Gaisford,  
375 3D Printing of a Multi-Layered Polypill Containing Six Drugs Using a Novel Stereolithographic  
376 Method, *Pharmaceutics*, 11 (2019).
- 377 [9] B.C. Pereira, A. Isreb, R.T. Forbes, F. Dores, R. Habashy, J.B. Petit, M.A. Alhnan, E.F. Oga,  
378 'Temporary Plasticiser': A novel solution to fabricate 3D printed patient-centred cardiovascular  
379 'Polypill' architectures, *European journal of pharmaceutics and biopharmaceutics : official journal of*  
380 *Arbeitsgemeinschaft fur Pharmazeutische Verfahrenstechnik e.V*, 135 (2019) 94-103.
- 381 [10] S.A. Khaled, J.C. Burley, M.R. Alexander, J. Yang, C.J. Roberts, 3D printing of five-in-one dose  
382 combination polypill with defined immediate and sustained release profiles, *Journal of controlled*  
383 *release : official journal of the Controlled Release Society*, 217 (2015) 308-314.
- 384 [11] A. Ajmal, A. Meskarzadeh, N. Genina, C. Hirschberg, J.P. Boetker, J. Rantanen, The Use of 3D  
385 Printed Molds to Cast Tablets with a Designed Disintegration Profile, *AAPS PharmSciTech*, 20 (2019)  
386 127.
- 387 [12] A. Goyanes, A.B. Buanz, A.W. Basit, S. Gaisford, Fused-filament 3D printing (3DP) for fabrication  
388 of tablets, *Int J Pharm*, 476 (2014) 88-92.
- 389 [13] H.E. Gultekin, S. Tort, F. Acarturk, An Effective Technology for the Development of Immediate  
390 Release Solid Dosage Forms Containing Low-Dose Drug: Fused Deposition Modeling 3D Printing,  
391 *Pharm Res*, 36 (2019) 128.
- 392 [14] Q. Li, H. Wen, D. Jia, X. Guan, H. Pan, Y. Yang, S. Yu, Z. Zhu, R. Xiang, W. Pan, Preparation and  
393 investigation of controlled-release glipizide novel oral device with three-dimensional printing, *Int J*  
394 *Pharm*, 525 (2017) 5-11.
- 395 [15] M. Saviano, R.P. Aquino, P. Del Gaudio, F. Sansone, P. Russo, Poly(vinyl alcohol) 3D printed  
396 tablets: The effect of polymer particle size on drug loading and process efficiency, *Int J Pharm*, 561  
397 (2019) 1-8.
- 398 [16] J. Skowyra, K. Pietrzak, M.A. Alhnan, Fabrication of extended-release patient-tailored  
399 prednisolone tablets via fused deposition modelling (FDM) 3D printing, *European journal of*  
400 *pharmaceutical sciences : official journal of the European Federation for Pharmaceutical Sciences*, 68  
401 (2015) 11-17.
- 402 [17] A. Goyanes, A.B. Buanz, G.B. Hatton, S. Gaisford, A.W. Basit, 3D printing of modified-release  
403 aminosaliclate (4-ASA and 5-ASA) tablets, *European journal of pharmaceutics and biopharmaceutics*  
404 *: official journal of Arbeitsgemeinschaft fur Pharmazeutische Verfahrenstechnik e.V*, 89 (2015) 157-  
405 162.

406 [18] J. Aho, J.P. Botker, N. Genina, M. Edinger, L. Arnfast, J. Rantanen, Roadmap to 3D-Printed Oral  
407 Pharmaceutical Dosage Forms: Feedstock Filament Properties and Characterization for Fused  
408 Deposition Modeling, *J Pharm Sci*, 108 (2019) 26-35.

409 [19] E. Fuenmayor, M. Forde, A.V. Healy, D.M. Devine, J.G. Lyons, C. McConville, I. Major, Material  
410 Considerations for Fused-Filament Fabrication of Solid Dosage Forms, *Pharmaceutics*, 10 (2018).

411 [20] J.M. Nasereddin, N. Wellner, M. Alhijaj, P. Belton, S. Qi, Development of a Simple Mechanical  
412 Screening Method for Predicting the Feedability of a Pharmaceutical FDM 3D Printing Filament,  
413 *Pharm Res*, 35 (2018) 151.

414 [21] T.C. Okwuosa, D. Stefaniak, B. Arafat, A. Isreb, K.W. Wan, M.A. Alhnan, A Lower Temperature  
415 FDM 3D Printing for the Manufacture of Patient-Specific Immediate Release Tablets, *Pharm Res*, 33  
416 (2016) 2704-2712.

417 [22] G. Kollamaram, D.M. Croker, G.M. Walker, A. Goyanes, A.W. Basit, S. Gaisford, Low temperature  
418 fused deposition modeling (FDM) 3D printing of thermolabile drugs, *Int J Pharm*, 545 (2018) 144-  
419 152.

420 [23] W. Kempin, V. Domsta, I. Brecht, B. Semmling, S. Tillmann, W. Weitschies, A. Seidlitz,  
421 Development of a dual extrusion printing technique for an acid- and thermo-labile drug, *European*  
422 *journal of pharmaceutical sciences : official journal of the European Federation for Pharmaceutical*  
423 *Sciences*, 123 (2018) 191-198.

424 [24] W. Kempin, V. Domsta, G. Grathoff, I. Brecht, B. Semmling, S. Tillmann, W. Weitschies, A.  
425 Seidlitz, Immediate Release 3D-Printed Tablets Produced Via Fused Deposition Modeling of a  
426 Thermo-Sensitive Drug, *Pharm Res*, 35 (2018) 124.

427 [25] S.A. Khaled, M.R. Alexander, D.J. Irvine, R.D. Wildman, M.J. Wallace, S. Sharpe, J. Yoo, C.J.  
428 Roberts, Extrusion 3D Printing of Paracetamol Tablets from a Single Formulation with Tunable  
429 Release Profiles Through Control of Tablet Geometry, *AAPS PharmSciTech*, 19 (2018) 3403-3413.

430 [26] S.A. Khaled, M.R. Alexander, R.D. Wildman, M.J. Wallace, S. Sharpe, J. Yoo, C.J. Roberts, 3D  
431 extrusion printing of high drug loading immediate release paracetamol tablets, *Int J Pharm*, 538  
432 (2018) 223-230.

433 [27] I.E. Aita, J. Breitzkreutz, J. Quodbach, Investigation of semi-solid formulations for 3D printing of  
434 drugs after prolonged storage to mimic real-life applications, *Eur J Pharm Sci*, 146 (2020) 105266.

435 [28] Q. Li, X. Guan, M. Cui, Z. Zhu, K. Chen, H. Wen, D. Jia, J. Hou, W. Xu, X. Yang, W. Pan, Preparation  
436 and investigation of novel gastro-floating tablets with 3D extrusion-based printing, *Int J Pharm*, 535  
437 (2018) 325-332.

438 [29] Z. Zheng, J. Lv, W. Yang, X. Pi, W. Lin, Z. Lin, W. Zhang, J. Pang, Y. Zeng, Z. Lv, H. Lao, Y. Chen, F.  
439 Yang, Preparation and application of subdivided tablets using 3D printing for precise hospital  
440 dispensing, *Eur J Pharm Sci*, 149 (2020) 105293.

441 [30] K. Vithani, A. Goyanes, V. Jannin, A.W. Basit, S. Gaisford, B.J. Boyd, A Proof of Concept for 3D  
442 Printing of Solid Lipid-Based Formulations of Poorly Water-Soluble Drugs to Control Formulation  
443 Dispersion Kinetics, *Pharm Res*, 36 (2019) 102.

444 [31] A. Goyanes, C.M. Madla, A. Umerji, G. Duran Pineiro, J.M. Giraldez Montero, M.J. Lamas Diaz,  
445 M. Gonzalez Barcia, F. Taherali, P. Sanchez-Pintos, M.L. Couce, S. Gaisford, A.W. Basit, Automated  
446 therapy preparation of isoleucine formulations using 3D printing for the treatment of MSUD: First  
447 single-centre, prospective, crossover study in patients, *Int J Pharm*, 567 (2019) 118497.

448 [32] A. Goyanes, N. Allahham, S.J. Trenfield, E. Stoyanov, S. Gaisford, A.W. Basit, Direct powder  
449 extrusion 3D printing: Fabrication of drug products using a novel single-step process, *Int J Pharm*,  
450 567 (2019) 118471.

451 [33] W. Grymonpre, W. De Jaeghere, E. Peeters, P. Adriaensens, J.P. Remon, C. Vervaet, The impact  
452 of hot-melt extrusion on the tableting behaviour of polyvinyl alcohol, *Int J Pharm*, 498 (2016) 254-  
453 262.

454 [34] Merck, Parteck MXP: Technical Informatiol, in, 2016.

455 [35] H.L. Ohrem, E. Schornick, A. Kalivoda, R. Ognibene, Why is mannitol becoming more and more  
456 popular as a pharmaceutical excipient in solid dosage forms?, *Pharm Dev Technol*, 19 (2014) 257-  
457 262.

458 [36] J. Quodbach, P. Kleinebudde, A critical review on tablet disintegration, *Pharm Dev Technol*, 21  
459 (2016) 763-774.

460 [37] P. Mura, M.T. Faucci, A. Manderioli, S. Furlanetto, S. Pinzauti, Thermal analysis as a screening  
461 technique in preformulation studies of picotamide solid dosage forms, *Drug Dev Ind Pharm*, 24  
462 (1998) 747-756.

463 [38] M. Mohsin, A. Hossin, Y. Haik, Thermomechanical properties of poly(vinyl alcohol) plasticized  
464 with varying ratios of sorbitol, *Mat Sci Eng a-Struct*, 528 (2011) 925-930.

465 [39] H.F. Tian, D. Liu, Y.Y. Yao, S.B. Ma, X. Zhang, A.M. Xiang, Effect of Sorbitol Plasticizer on the  
466 Structure and Properties of Melt Processed Polyvinyl Alcohol Films, *J Food Sci*, 82 (2017) 2926-2932.

467 [40] A. Isreb, K. Baj, M. Wojsz, M. Isreb, M. Peak, M.A. Alhnan, 3D printed oral theophylline doses  
468 with innovative 'radiator-like' design: Impact of polyethylene oxide (PEO) molecular weight, *Int J*  
469 *Pharm*, 564 (2019) 98-105.

470 [41] M. Sadia, A. Sosnicka, B. Arafat, A. Isreb, W. Ahmed, A. Kelarakis, M.A. Alhnan, Adaptation of  
471 pharmaceutical excipients to FDM 3D printing for the fabrication of patient-tailored immediate  
472 release tablets, *Int J Pharm*, 513 (2016) 659-668.

473 [42] B.C. Pereira, A. Isreb, M. Isreb, E.F. Forbes, E.F. Oga, M.A. Alhnan, Additive manufacturing of a  
474 point-of-care "polypill": Fabrication of concept capsules of complex geometry with bespoke release  
475 against cardiovascular disease *Advanced Healthcare Materials*, (Accepted) (2020).

476 [43] M. Sadia, B. Arafat, W. Ahmed, R.T. Forbes, M.A. Alhnan, Channelled tablets: An innovative  
477 approach to accelerating drug release from 3D printed tablets, *J Control Release*, 269 (2018) 355-  
478 363.

479 [44] J.S. Wilkhu, S.E. McNeil, D.E. Anderson, M. Kirchmeier, Y. Perrie, Development of a solid dosage  
480 platform for the oral delivery of bilayer vesicles, *European journal of pharmaceutical sciences* :  
481 official journal of the European Federation for Pharmaceutical Sciences, 108 (2017) 71-77.

482 [45] A.H. Ibrahim, E. Rosqvist, J.H. Smatt, H.M. Ibrahim, H.R. Ismael, M.I. Afouna, A.M. Samy, J.M.  
483 Rosenholm, Formulation and optimization of lyophilized nanosuspension tablets to improve the  
484 physicochemical properties and provide immediate release of silymarin, *International Journal of*  
485 *Pharmaceutics*, 563 (2019) 217-227.

486 [46] G.A. Gonzalez Novoa, J. Heinamaki, S. Mirza, O. Antikainen, A.I. Colarte, A.S. Paz, J. Yliruusi,  
487 Physical solid-state properties and dissolution of sustained-release matrices of polyvinylacetate, *Eur*  
488 *J Pharm Biopharm*, 59 (2005) 343-350.

489 [47] J.E.M. Snaar, R. Bowtell, C.D. Melia, S. Morgan, B. Narasimhan, N.A. Peppas, Self-diffusion and  
490 molecular mobility in PVA-based dissolution-controlled systems for drug delivery, *Magnetic*  
491 *Resonance Imaging*, 16 (1998) 691-694.

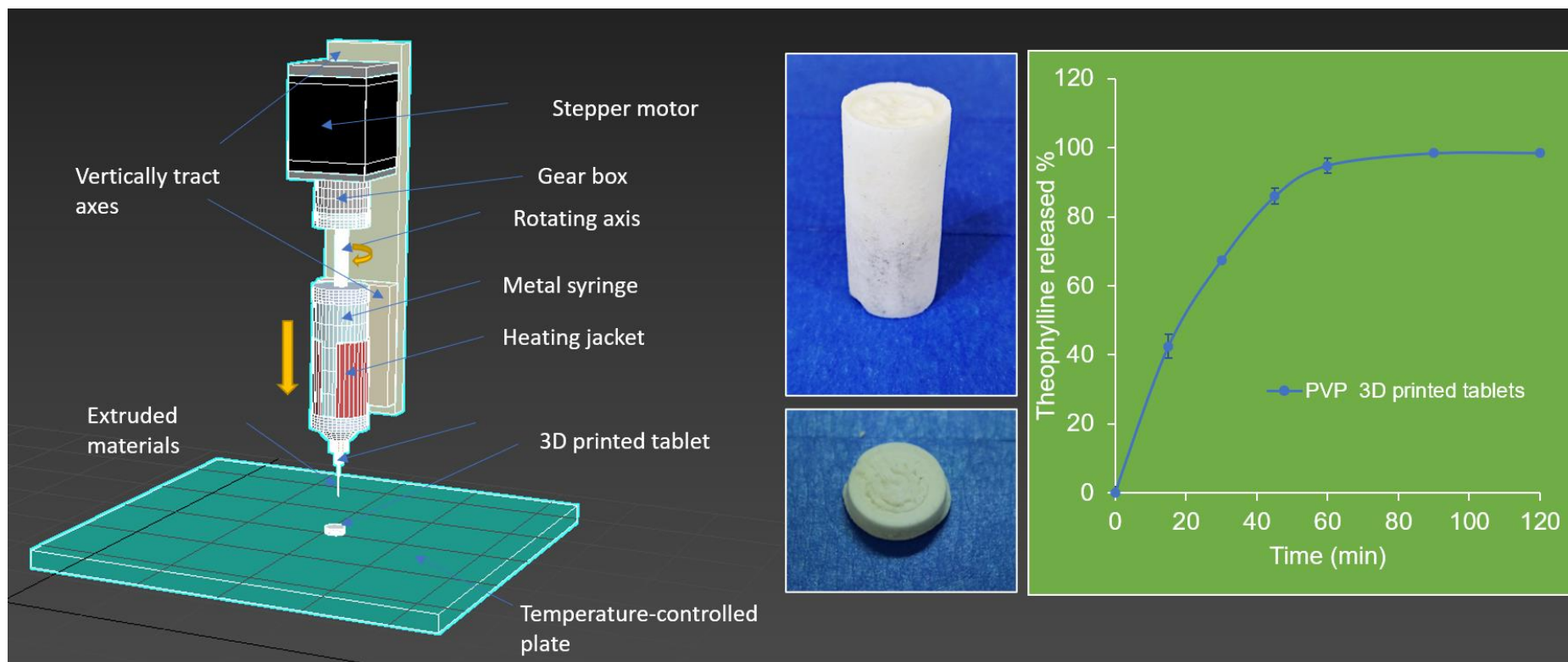
492 [48] E. Karavas, E. Georgarakis, M.P. Sigalas, K. Avgoustakis, D. Bikiaris, Investigation of the release  
493 mechanism of a sparingly water-soluble drug from solid dispersions in hydrophilic carriers based on  
494 physical state of drug, particle size distribution and drug-polymer interactions, *Eur J Pharm*  
495 *Biopharm*, 66 (2007) 334-347.

496 [49] F.I. Kanaze, E. Kokkalou, I. Niopas, M. Georgarakis, A. Stergiou, D. Bikiaris, Dissolution  
497 enhancement of flavonoids by solid dispersion in PVP and PEG matrixes: A comparative study, *J Appl*  
498 *Polym Sci*, 102 (2006) 460-471.

499 [50] T.C. Okwuosa, B.C. Pereira, B. Arafat, M. Cieszynska, A. Isreb, M.A. Alhnan, Fabricating a Shell-  
500 Core Delayed Release Tablet Using Dual FDM 3D Printing for Patient-Centred Therapy, *Pharm Res*, 34  
501 (2017) 427-437.

502 [51] B. Arafat, M. Wojsz, A. Isreb, R.T. Forbes, M. Isreb, W. Ahmed, T. Arafat, M.A. Alhnan, Tablet  
503 fragmentation without a disintegrant: A novel design approach for accelerating disintegration and  
504 drug release from 3D printed cellulosic tablets, *Eur J Pharm Sci*, 118 (2018) 191-199.

505

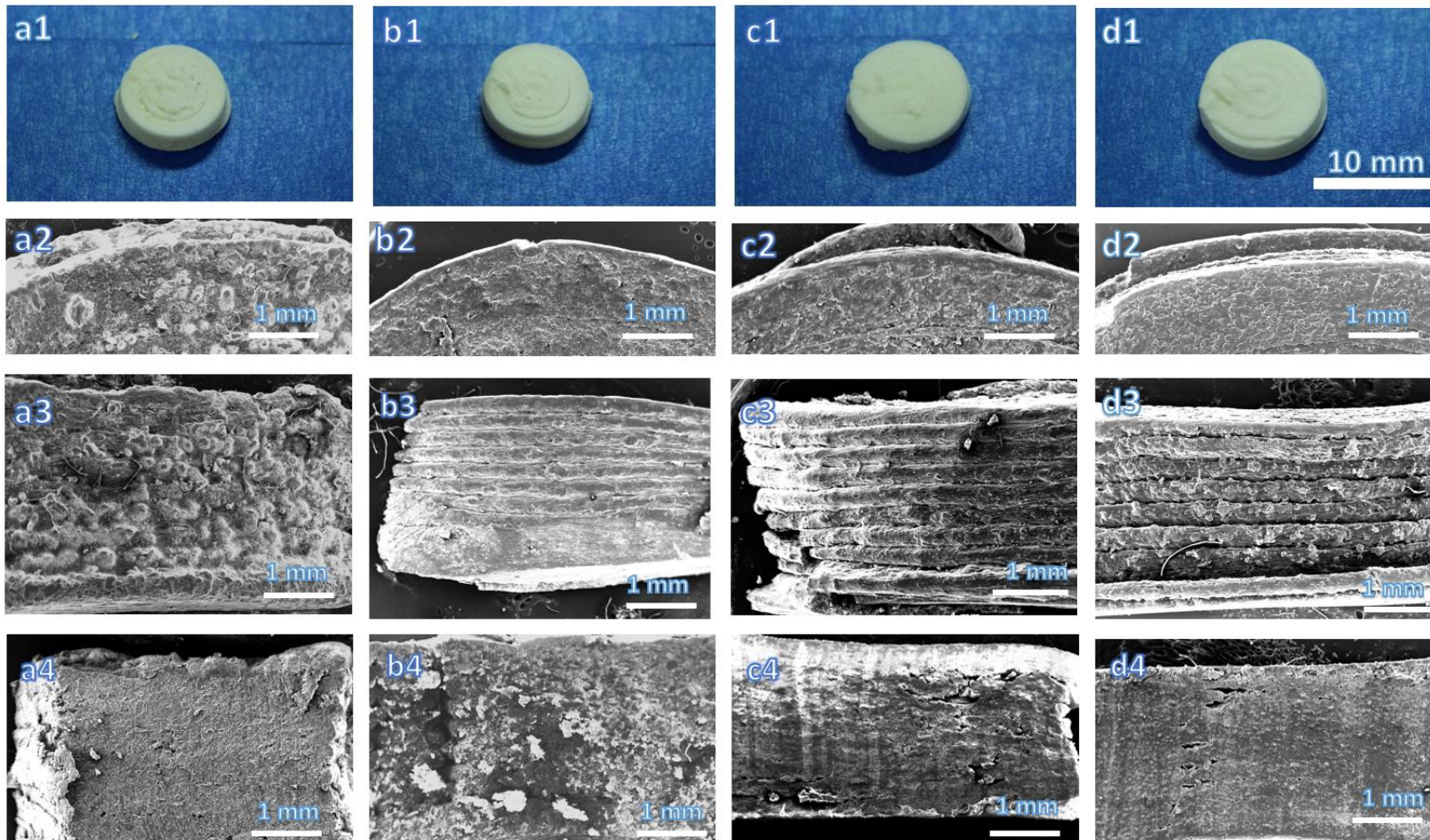


506

507 **Fig. 1.** Equipment for TASFEX 3D printing. (a) The printer is equipped with a metal syringe surrounded by temperature-controlled heating jacket. The syringe  
 508 is fitted with a luer-lock stainless steel needle, (b) The pharmaceutical ink (compressed powder) is added. The ink is then extruded by a piston pushed by  
 509 computer-controlled stepper motor equipped with gear to produce (c) 3D printed tablet.

510

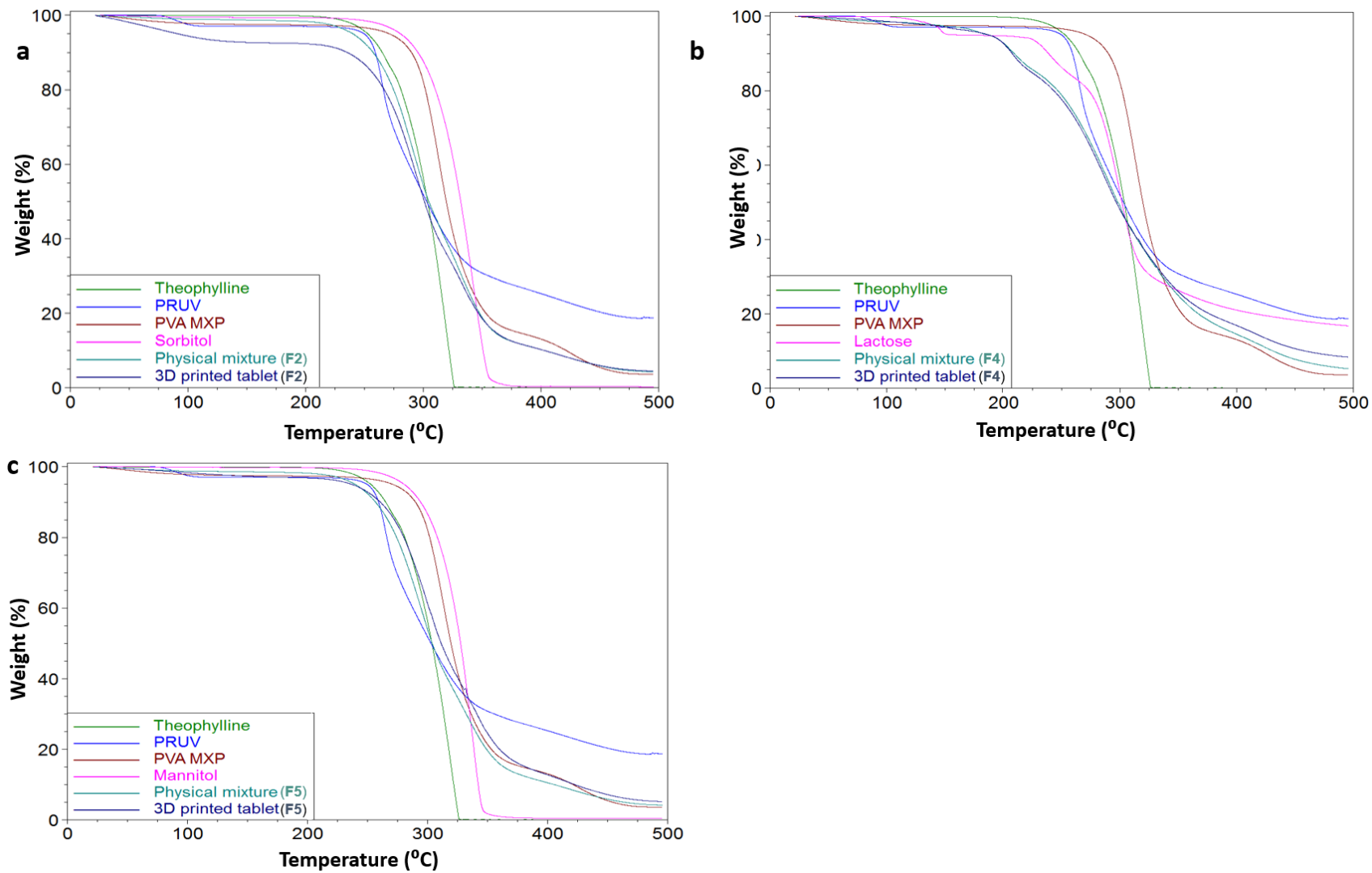




511

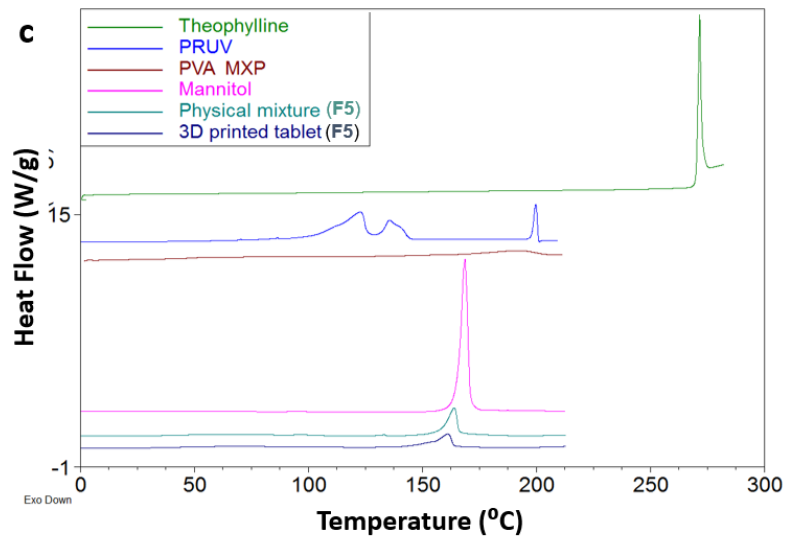
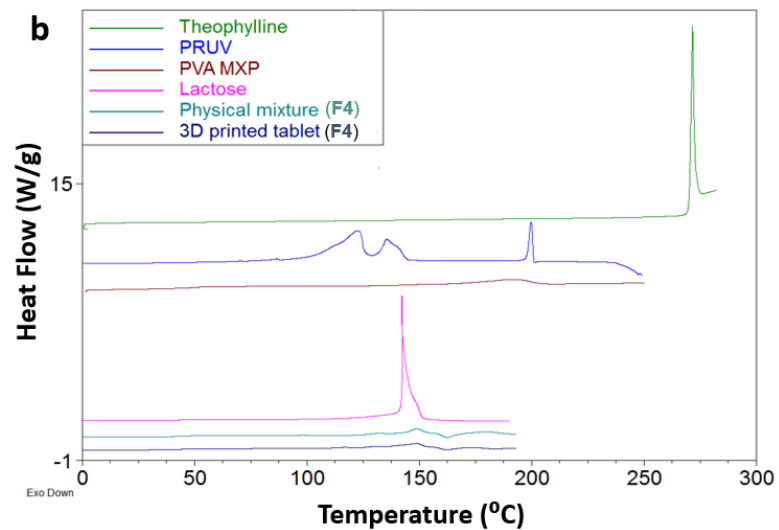
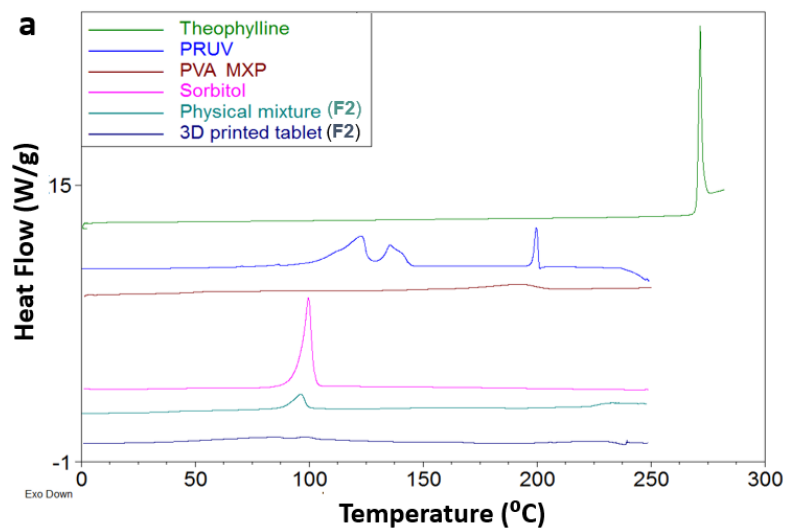
512 **Fig. 2** Photographs of 3D printed tablets based on (a1) PVA and sorbitol, (b1) PVA and lactose and (c1) PVA and D-mannitol and (d1) PVP and lactose. SEM  
 513 images of (a2, b2, c2 and d2) top view, (a3, b3, c3 and d3) side view, and (a4, b4, c4 and d4) cross sections of these tablets.

514



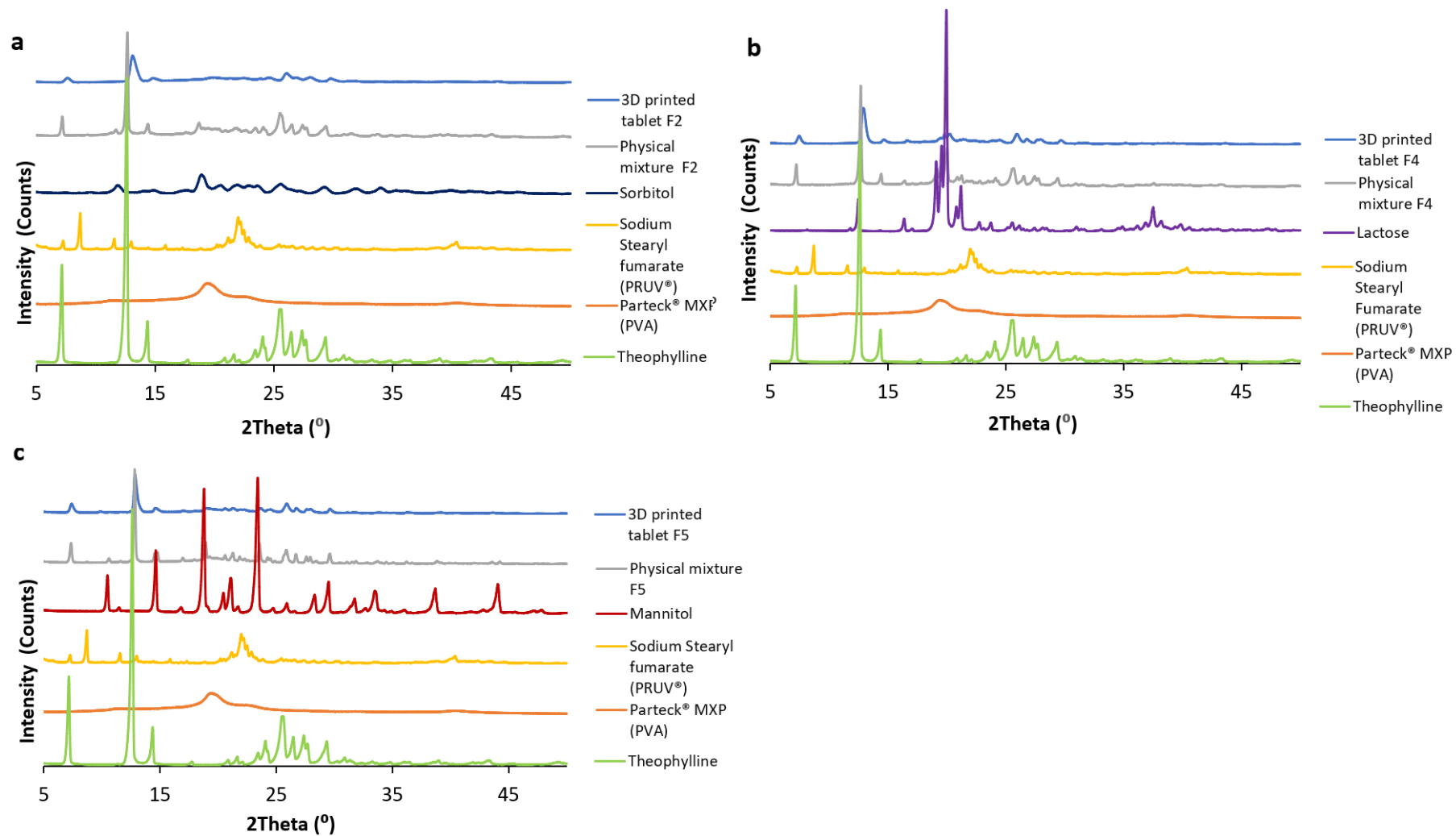
515

516 **Fig. 3** TGA thermal degradation profiles of raw theophylline, PVA, Sodium stearyl fumarate (PRUV), filler [ (a) sorbitol, (b) lactose and (c) D-mannitol],  
 517 pharmaceutical ink (prior to addition of water) and 3D printed tablets.



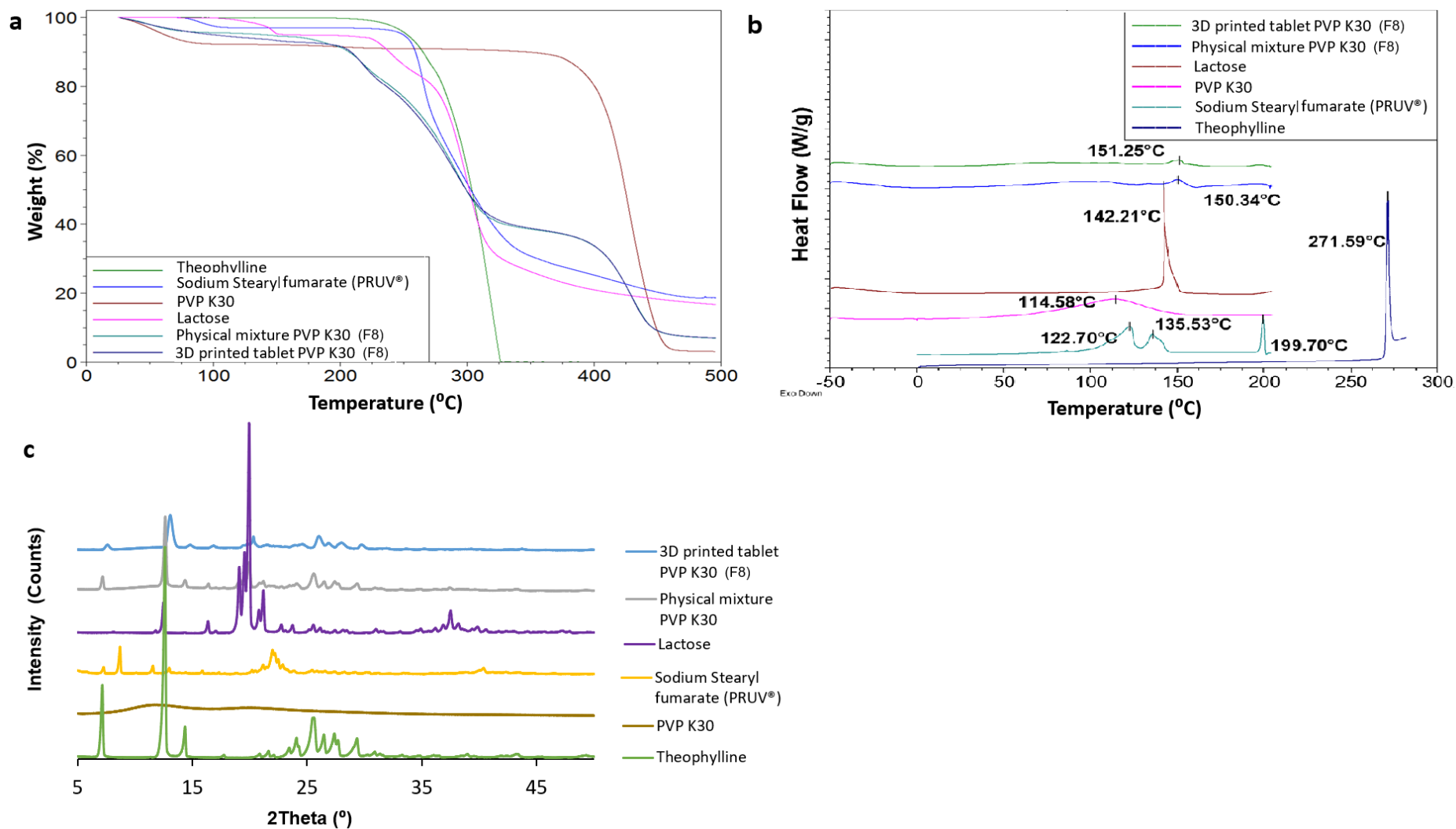
518

519 **Fig. 4** DSC thermograph of raw theophylline, PVA, Sodium stearyl fumarate (PRUV), filler [(a) sorbitol, (b) lactose and (c) D-mannitol], pharmaceutical ink  
 520 (prior to addition of water) and 3D printed tablets.



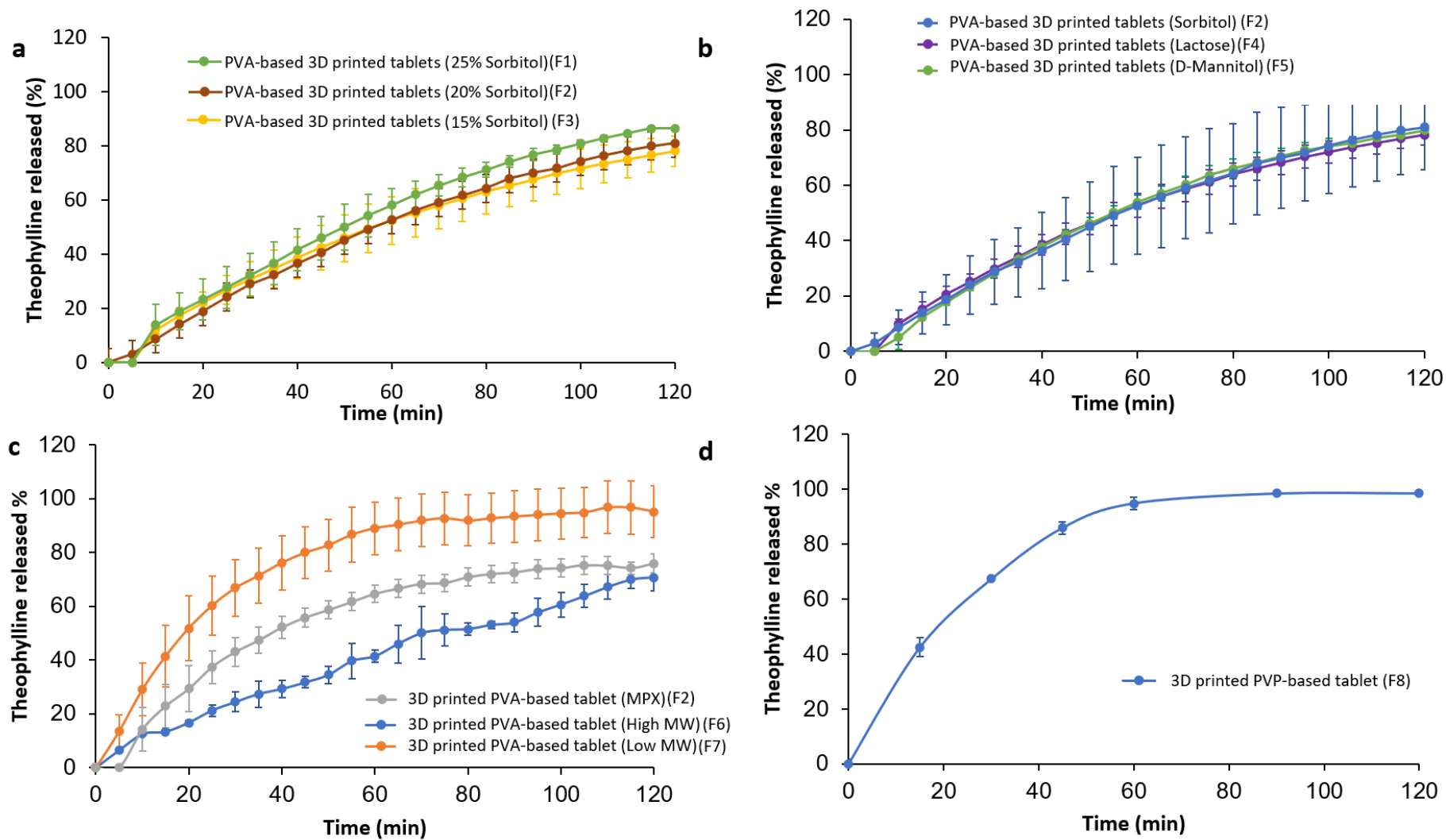
521

522 **Fig. 5** XRD patterns of raw theophylline, PVA, Sodium stearyl fumarate (PRUV), filler [ (a) sorbitol, (b) lactose and (c) D-mannitol, pharmaceutical ink (prior  
 523 to addition of water) and 3D printed tablets.



524

525 **Fig. 6** 3D Printed tablet based on poly(vinylpyridine) (PVP) (A) TGA thermal degradation profiles, (B) DSC thermograph profiles, (C) XRD patterns of raw  
 526 theophylline, PVP, Sodium stearyl fumarate (PRUV), lactose, pharmaceutical ink (prior to addition of water) and 3D printed tablets.



527

528 **Fig. 7** Impact of (a) sorbitol percentage, (b) nature of filler (sorbitol, lactose and D-mannitol), and (c) molecular weight of PVA on the *in vitro* dissolution of  
 529 theophylline from 3D printed tablets, (d) *in vitro* dissolution of theophylline from 3D printed PVP based tablets (n= 3,  $\pm$ SD).